Eur. Phys. J. D **8**, 277–286 (2000)

THE EUROPEAN PHYSICAL JOURNAL D

EDP Sciences

Laser capabilities of CuBr mixture excited by RF discharge

M. Grozeva[1,a], M. Kocik[2], J. Mentel[3], J. Mizeraczyk[2], T. Petrov[1], P. Telbizov[1], D. Teuner[3], N. Sabotinov[1], and J. Schulze[3]

[1] Institute of Solid State Physics, Bulgarian Academy of Sciences, Tzarigradsko Chausse 72, 1784 Sofia, Bulgaria
[2] Institute of Fluid Flow Machinery, Polish Academy of Sciences, Fiszera 14, 80-952 Gdańsk, Poland
[3] Department of Electrotechnical Engineering, Ruhr-University, Universitätsstraße 150, 44780 Bochum, Germany

Received 4 January 1999

Abstract. Our investigations demonstrated that utilizing copper bromide (CuBr) mixture as a source of Cu atoms in a RF-excited discharge can be a promising alternative to the Cu sputtered system, when the development of Cu ion gas laser is considered. Both spectroscopic and laser investigations showed that the threshold input power for lasing was reduced about 5 times using the CuBr-based system instead of the Cu-sputtered system. Pulsed and CW laser oscillation on Cu^+ transitions in the near IR spectral region was obtained in RF-excited He–CuBr discharge operated at 13.56 MHz and 27.12 MHz. At input RF power of 800 W, a laser output power of 10 mW at the 780.8 nm Cu ion laser line was achieved. An increase of laser output power by a factor of two, as well as better Cu vapour axial distribution and better discharge stability, was attained when DC discharge was superimposed on the RF discharge. Laser gain on 11 UV Cu ion lines was observed in RF-excited Ne–CuBr discharge. basing on the obtained results, we consider the CuBr laser system excited by RF discharge capable of generating UV laser radiation at relatively low input power.

PACS. 42.60.By Design of specific laser systems – 42.55.Lt Gas lasers including excimer and metal-vapor lasers – 52.80.Pi High-frequency discharges

1 Introduction

The copper ion (Cu^+) laser is one of the most efficient metal ion lasers, capable of generating CW laser lines in a wide spectral range extending from the near IR to the deep UV (54 laser lines in total, 11 of them in the UV, [1]). Two methods have been employed for producing the laser medium with Cu^+ ions excited to the upper laser levels. In the first method, discharge sputtering of the copper electrode is used to produce free Cu atoms, which then are ionised and excited to the upper laser levels. The Cu^+ lasers excited with this method are called the *sputtered copper ion lasers*. However, in the sputtered Cu^+ lasers a rather high input power (more than 100 W/cm, [2,3]) is necessary to obtain the required Cu atoms density in the laser medium. An alternative method for producing free Cu atoms in the laser medium is to seed the discharge with a copper halide (*e.g.* copper bromide), similarly to the pulsed selfterminating metal vapour lasers [4–6]. The Cu^+ lasers employing copper halides as a source of Cu atoms are called the *halide-based copper ion lasers*.

In the sputtered Cu^+ lasers a *hollow cathode (HC) and a radio frequency (RF) discharge* have been used for sputtering the copper electrode to obtain free Cu atoms in the laser medium.

[a] e-mail: margo@issp.bas.bg

Laser output power of about 1 W at CW operation and about 5 W at quasi CW operation (pulse duration of 100 μs, repetition rate of 40 Hz) have been reached at 780 nm in the sputtered Cu^+ lasers excited by HC discharge [7]. The record value of the laser output power in the UV region around 260 nm is about 900 mW under multiline operation [8]. This makes the Cu^+ lasers very attractive for various applications in biology, medicine, microelectronics, etc. However, to make the HC discharge-excited Cu^+ laser a practical device a lot of problems exist connected with the poor stability of the HC discharge, short life-time, complicated and expensive design of the discharge tube, etc.

It has been demonstrated that many ionic laser lines, which can be generated in a HC discharge, can be also efficiently excited in a RF discharge, in particular in a capacitively coupled RF discharge (see, *e.g.* [9]). The capacitively coupled RF discharge excitation [9–12] offers high longitudinal homogeneity of the discharge, more efficient transforming of the input power into energy of the fast electrons, better stability of the discharge, less complicated laser tube design and possibility of using external electrodes. These advantages have been recently demonstrated by the efficient CW operation of RF-excited He–Cd^+ and He–Kr^+ lasers [11,12].

Laser oscillation in a pulsed mode on near IR Cu^+ lines excited in a RF discharge was reported first by Mikhalevskii *et al.* [13]. To produce the density of Cu atoms necessary for lasing, they used the sputtering of an internal copper electrode in a transverse RF He–Cu discharge excited with a RF power of 2 kW (corresponding to about 100 W per 1 cm of the sputtered electrode). Also our results showed that an input power higher than 100 W/cm is needed for efficient production of Cu atoms in the sputtered Cu^+ lasers excited by RF discharge [14,15].

The idea of using a copper halide as a source of copper atoms in the HC-excited Cu^+ lasers, to avoid the high input power which is necessary for producing the appropriate copper atom density in the sputtered laser systems, was introduced by Piper and Neely [16]. The introduction of a copper halide as an impurity to the HC discharge without deterioration of the discharge was possible owing to the relatively high density of fast electrons the HC discharge, which makes the HC discharge insensitive to the presence of such impurity in the operating gas. Using copper halides (CuCl, CuBr, CuI) Piper and Neely obtained laser oscillation in the HC discharge on several near IR Cu^+ transitions reducing the threshold current for lasing by a factor of 2–3 in respect to that typical of the sputtered Cu^+ laser excited in a HC discharge.

In the halide-based Cu^+ lasers the required copper vapour density is produced by discharge dissociation of the copper halide molecules introduced into the discharge volume by thermal evaporation of the copper halide powder. As the fractional dissociation of molecules in the discharge volume saturates at a relatively low discharge current, the free Cu atom density is independent of the discharge current under normal operating conditions and can be optimised separately by controlling the thermal evaporation of the copper halide powder.

In this paper we report results of applying copper bromide (CuBr) as a source of Cu atoms in a RF-excited Cu^+ laser. Laser oscillations on Cu^+ transitions in the near IR spectral region were obtained in the He–CuBr discharge at pulsed and CW excitation. Laser gain on several UV Cu^+ lines was observed in the Ne–CuBr discharge. The power consumed for the excitation of Cu^+ lines was determined. To determine the discharge conditions optimal for efficient excitation of the Cu^+ lines we made some spectroscopic investigations of the He(Ne)–CuBr discharge at different RF input powers. These investigations gave also information about the changes in the operating gas during the discharge operation (formation and accumulation of Br_2 and other molecules in and outside the discharge) and their influence on the excitation of the laser lines.

2 Plasma processes in RF discharge in He(Ne)-CuBr mixtures

It is recognised that efficient excitation of the upper laser levels of Cu^+ ions occurs in the charge-transfer processes [17]

$$He^+ + Cu \rightarrow He + Cu^{+*} \quad (1)$$

or

$$Ne^+ + Cu \rightarrow Ne + Cu^{+*}. \quad (2)$$

The plasma of the RF-excited He(Ne)–CuBr discharge, similarly to that of the HC discharge exhibits characteristics favourable for efficient realisation of reactions (1, 2). First, in both discharges, RF and HC in He(Ne)–CuBr mixtures [18,19] the density of the slow (or plasma) electrons characterised by a mean energy of about 0.5 eV is high [20], so enough electrons with sufficient energy to induce dissociation by direct impact are present in the discharge. Therefore, in both discharges efficient dissociation of CuBr molecules (dissociation energy 3.4 eV, [21]) *via* collisions with relatively slow electrons occurs. Owing to it free Cu atoms are produced from CuBr molecules in the discharge region. Second, in both discharges a large number of fast electrons (with energy above 20 eV and a local maximum around 26 eV) exists [20,22–24]. These fast electrons are capable of ionising He or Ne atoms, necessary for efficient realisation of the reactions (1, 2).

The Cu^+ ions recombine in the discharge volume by collisions with electrons or halogen ions, or at the tube wall, to generate neutral ground-state Cu atoms. Then they may combine with Br atoms or molecules, forming CuBr compounds. For efficient Cu^+ laser operation it is important that the dissociation of CuBr molecules and the subsequent excitation of the thus produced Cu atoms to the upper laser levels, is accompanied by chemical recombination of the CuBr dissociation products to re-form the donor CuBr molecules.

The efficiency of the recombination of Cu and Br molecules strongly depends on temperature and above 820 K a breakdown in the recombination process is observed [16]. Therefore, for efficient operation of halide-based Cu^+ lasers the discharge tube temperature should be kept below 820 K. At working temperature below 820 K the discharge tube wall is "cold" for the Cu atoms, and those Cu atoms which fail to recombine with Br atoms in the discharge volume deposit on the tube wall. Practically, full recombination of the Cu and Br atoms in the discharge volume cannot occur to form the original compound. Therefore after some period of the laser operation copper deposits are observed on the tube wall in the discharge region. The copper deposit means that an excess of free Br atoms exists first in the discharge and then, due to diffusion, in the off-discharge parts of the laser tube.

The presence of bromine in the laser tube can have negative effects on the laser operation. First, bromine is chemically very active and may deteriorate the metal parts of the laser tube. Also, due to the bromine activity, some interaction of Br atoms with the silica tube may occur at high temperature, resulting in the production of SiBr molecules that can be present in the operating gas and can absorb or scatter the generated laser radiation [25]. It is known that SiBr molecules have absorption bands below 300 nm [21]. The formation of SiBr molecules seems

to be more probable in a RF-excited discharge, which sputters the silica tube wall with high efficiency [12]. It is possible that some SiO and BrO molecules are also formed in the RF-excited discharge. Second, bromine tends to combine in Br_2 molecules. However, in the discharge region there are practically no Br_2 molecules because of their efficient dissociation *via* collisions with electrons (dissociation energy of Br_2 is ~ 2 eV [26]). On the other hand, Br_2 molecules accumulate in the cold regions of the laser tube, as it was found in a pulsed selfterminated CuBr laser [27], having buffer gas pressure and working temperature similar to the halide-based Cu^+ lasers. Presence of Br_2 molecules in the laser discharge tube may deteriorate the laser operation due to instabilities of the discharge and absorption of the laser lines.

On the other hand, it is known [26] that the main absorption continuum of Br_2 molecules is in the blue spectral region, from 300 nm to 510 nm with a maximum around 430 nm, so we should not expect strong absorption losses due to the presence of Br_2 in the UV range below 300 nm. However, a weak absorption continuum was found in the 156 nm ÷ 300 nm range [26], as well as some narrow absorption bands of Br atoms in the UV region around 245 nm and 280 nm [21]. According to [25] the bromine spectrum between 200 nm ÷ 300 nm shows a relatively weak absorption at room temperature, but when increasing the temperature above 650 K the absorption slowly increases. Some narrow absorption bands of bromine are reported also in the ranges of 510 nm ÷ 640 nm and 645 nm ÷ 815 nm [25]. Even weak absorption by Br_2 molecules might be very critical for operation of the Cu^+ laser in the UV region because of the relatively low laser gain [7] in this spectral region. However, at the discharge conditions of a pulsed selfterminated CuBr laser [27] the absorption of Br_2 molecules was found only in the visible range without any effect on the output laser power of the high gain CuBr laser lines ($\lambda = 501.6$ nm and $\lambda = 578.2$ nm). Unfortunately, there is no information about the absorption in the UV and in the IR spectral regions where most of the Cu^+ ion laser lines belong. To clarify the influence of the present in the discharge species on the excitation of the Cu^+ laser lines we made spectroscopic measurements of the emission spectra of the He(Ne)–CuBr mixture at appropriate for laser oscillation discharge conditions.

3 Spectroscopic study of a RF discharge in a He(Ne)–CuBr mixtures

The experimental discharge tube was made of fused silica (Fig. 1). The 10 cm-long active part of the tube had an inner diameter of 8 mm. The buffer gas was He or Ne. In the middle of the discharge region a fused silica reservoir with CuBr pellets was placed. Distilled in vacuum 98% pure p.a. CuBr was used. The temperature of the CuBr reservoir was controlled by an external oven. Due to it, CuBr vapour pressure in the discharge volume was controlled independently from the RF power dissipated in the discharge. The RF power from a 13.56 MHz generator was capacitively coupled into the discharge with two brass electrodes (10 cm long, 8 mm wide) mounted along the active part of the tube. The RF power could be modulated and delivered to the discharge as pulses. The width and repetition rate of the pulses could be varied. It allowed to run the discharge at higher peak RF input power keeping the average power, and hence, the tube temperature in acceptable limits.

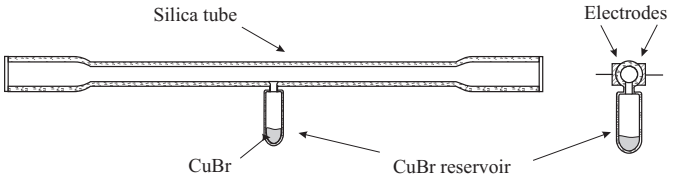

Fig. 1. Discharge tube used for the spectroscopic studies of the RF-excited He(Ne)–CuBr discharges.

The light emitted by the RF discharge in the He(Ne)–CuBr mixtures was collimated onto the entrance slit of a computer controlled 0.275 m digital scanning monochromator (Spectra-Pro, Acton Research Corporation) having spectral resolution better than 0.1 nm. The signal was recorded by an optical simultaneous multichannel analyser. The emission spectra in the 740 ÷ 800 nm spectral range of the He–CuBr discharge and in the 240 ÷ 300 nm spectral range of the Ne–CuBr discharge were recorded at different peak RF input powers (up to 400 W) and temperatures of the CuBr reservoir (up to 800 K).

The measurements showed that Br atomic lines appeared in the emission spectra of the He–CuBr discharge in the 740 nm ÷ 800 nm IR range when peak RF input power exceeded 100 W (corresponding to 10 W/cm). Their intensity increased with increasing CuBr reservoir temperature. Above 450 K Cu atomic line $\lambda = 793.3$ nm was also found in the emission spectrum and its intensity increased with increasing CuBr reservoir temperature. However, at 100 W RF input power no Cu^+ lines were found in the He–CuBr discharge emission spectrum at reservoir temperature as high as 800 K. When increasing the RF input power to 200 W (20 W/cm), weak Cu^+ lines were detected at a CuBr reservoir temperature of 650 K. Their intensity increased about 5 times when the CuBr reservoir temperature was increased up to 800 K. The emission spectrum of the RF-excited He–CuBr discharge at a He pressure of 3.0 kPa, CuBr reservoir temperature of 770 K and RF input power of 200 W is presented in Figure 2. As it is seen, in addition to He, Cu and Br atomic lines eight Cu^+ ion laser lines were detected. After cooling the CuBr reservoir to room temperature, several Br atomic lines were still present in the emission spectrum, indicating the presence of Br atoms in the discharge.

The emission spectrum of the Ne–CuBr discharge in the 240–300 nm spectral region exhibited the same dependence on CuBr vapour pressure like that of the He–CuBr discharge. At 100 W RF input power there were no atomic or ionic copper lines in the emission spectrum even when increasing the CuBr reservoir temperature up to 800 K.

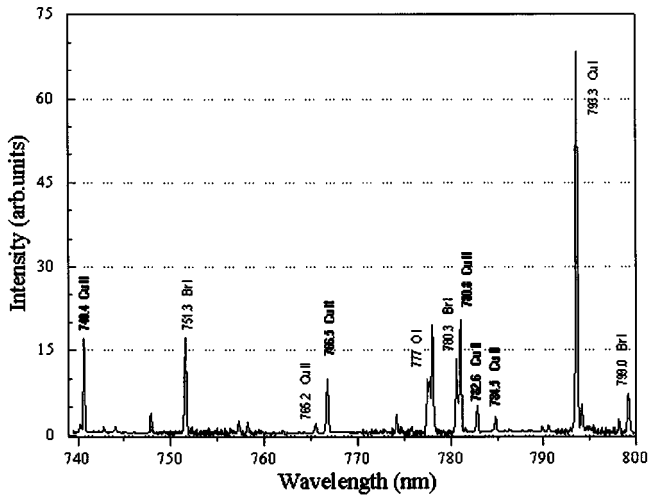

Fig. 2. Emission spectrum of the RF-excited He–CuBr discharge at 3.0 kPa He pressure, 770 K CuBr reservoir temperature and 200 W RF (13.56 MHz) input power. Cu^+ laser lines are marked bold.

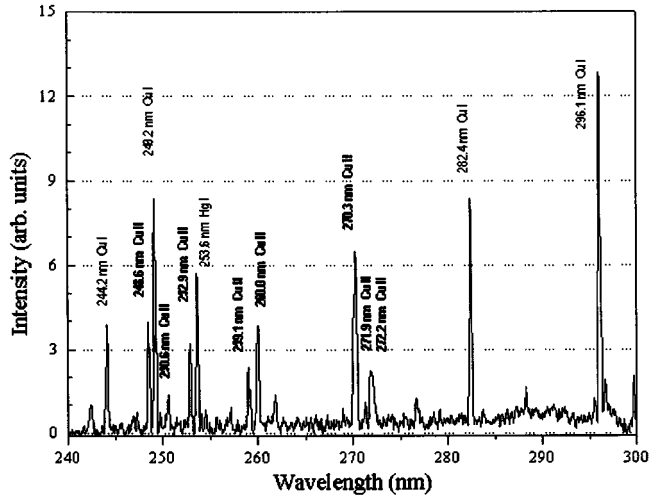

Fig. 3. Emission spectrum of the RF-excited Ne–CuBr discharge at 3.0 kPa Ne pressure, 770 K CuBr reservoir temperature and 200 W RF (13.56 MHz) input power. Cu^+ laser lines are marked bold.

At an RF input power of 200 W four Cu atomic lines and eight laser Cu^+ ion lines were detected (Fig. 3).

Simultaneously with the radiation emitted by the RF-excited discharge we recorded the intensity of the 253.7 nm Hg atomic line, emitted by a Hg lamp placed at the end-side of the discharge tube, and transmitted through the tube. The intensity of the 253.7 nm Hg atomic line decreased when increasing CuBr vapour pressure in the discharge. At temperature of the CuBr reservoir of 800 K the 253.7 nm Hg line intensity was about 20% lower than at room temperature. After cooling down the CuBr reservoir to room temperature the 253.7 nm Hg line recovered its initial intensity. This suggests that the 253.7 nm Hg line intensity suffered some losses in the RF-excited He–CuBr discharge due to absorption or scattering by Br_2 or other molecules. Then, after several hours of the discharge operation with the CuBr reservoir cooled down many intense molecular emission bands were detected (Fig. 4). These molecular bands were not present before in the emission spectra. Their appearance indicates that some changes in the composition of the gas mixture occurred. The intensity of 447.2 nm, 492.2 nm and 501.6 nm He atomic lines decreased twice, compared to their initial values, presumably due to either Br_2 absorption in the blue-green region [21,26] or plasma parameters changes, caused by the presence of bromine in the discharge.

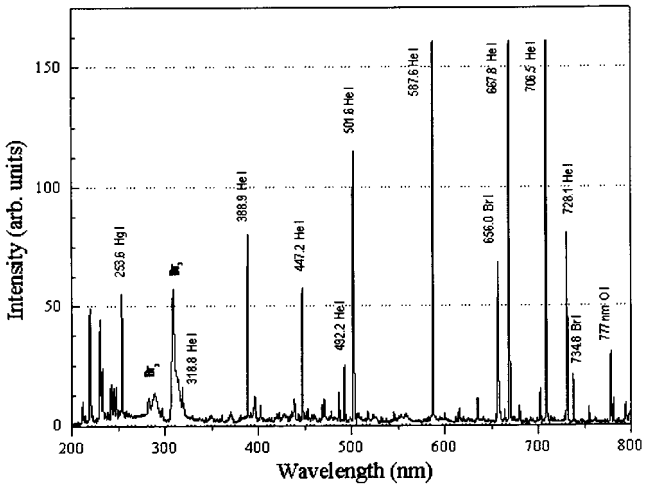

Fig. 4. Emission spectrum of the RF-excited He–CuBr discharge at 3.0 kPa He pressure, 300 K CuBr reservoir temperature and 100 W RF (13.56 MHz) input power. Br_2 bands are marked bold.

Our spectroscopic measurements of the RF-excited He(Ne)–CuBr discharge showed that efficient excitation of the Cu^+ laser lines may be obtained, if the RF input power exceeds 100 W at 10 cm active discharge length, *i.e.* at a linear RF input power density higher than 10 W/cm. At a lower RF input power, in spite of the presence of Cu atoms in the discharge, spontaneous emission of Cu^+ lines was not detected by us. Except for the Cu^+ laser lines, no other Cu^+ lines were found in the measured emission spectra even at an RF input power higher than 200 W. It proves that efficient charge-exchange excitation (reactions (1, 2)) takes place in the RF-excited He(Ne)–CuBr discharge at the examined conditions.

4 IR laser oscillations on Cu^+ lines in RF-excited He–CuBr discharges

4.1 RF-excitation and matching

RF power of two different frequencies was used for exciting the RF discharges in the He–CuBr mixtures, 13.56 MHz delivered by a generator of maximum output power of 1000 W and 27.12 MHz with maximum power of 2.5 kW. There was a possibility to modulate the RF power to get

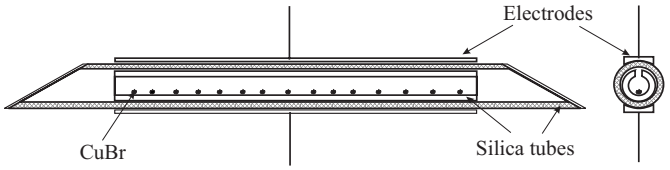

Fig. 5. RF-excited He–CuBr laser tube heated by the discharge.

trains of RF power pulses with variable repetition rate and pulse duration. Special circuits were developed to match the discharge impedance to the impedance of each RF generator. The matching circuits symmetrised the RF voltage and helped in maintaining uniform discharge between the electrodes and in avoiding strong RF interference [28]. The RF power was coupled into the discharge by two nickel-plated brass electrodes externally mounted along the opposite sides of the discharge tube.

4.2 "Pulsed" IR laser generation in He–CuBr discharge

Laser oscillation on the 780.8 nm Cu^+ transition in a RF-excited He–CuBr discharge in a "pulsed" regime was studied first. The He–CuBr discharge was excited by 27.12 MHz train pulses with a repetition rate and pulse duration varied from 1 kHz to 4 kHz and from 40 μs to 120 μs, respectively. The electrodes coupling the RF power into the discharge were 400 mm long and 8 mm wide. The laser tube was formed by two tubes, outer and inner. Both were made of fused silica (Fig. 5). The outer tube had an inner diameter of 8 mm and active length of 400 mm. The inner tube was 400 mm in length and 5.5 mm in bore diameter. Along the length of the inner tube a 4 mm slot was cut. Small solid pieces of CuBr halide were evenly distributed on the bottom of the inner tube along the slot. To evaporate the halide the discharge heating was used. The role of the inner tube was to prevent copper deposition on the inner surface of the outer discharge tube, since the copper deposits are usually a reason of electrical short-circuits.

The pulsed laser generation at $\lambda = 780.8$ nm Cu^+ was obtained at He pressures from 1.8 kPa to 5 kPa with an optimum at 4 kPa. The He pressure dependence (Fig. 6) was obtained at a constant RF pulses amplitude of 750 W and different temperatures of the discharge tube, optimal for each He pressure. The optimal discharge tube temperature measured at the surface of the outer discharge tube was 400 K at 1.8 kPa and increased to 450 K at 5 kPa He. The tube temperature was varied by changing the average RF input power through either pulse repetition rate or pulse duration at constant pulse amplitude.

A typical relation between the RF excitation and laser pulses at $\lambda = 780.8$ nm Cu^+ is shown in Figure 7. The laser pulse was delayed about $20 \div 60$ μs in respect to the RF excitation pulse. The delay time was dependent on the discharge conditions. It was shorter at lower He pressure and higher excitation pulse amplitude. We believe that this delay is attributed to the slow build up of

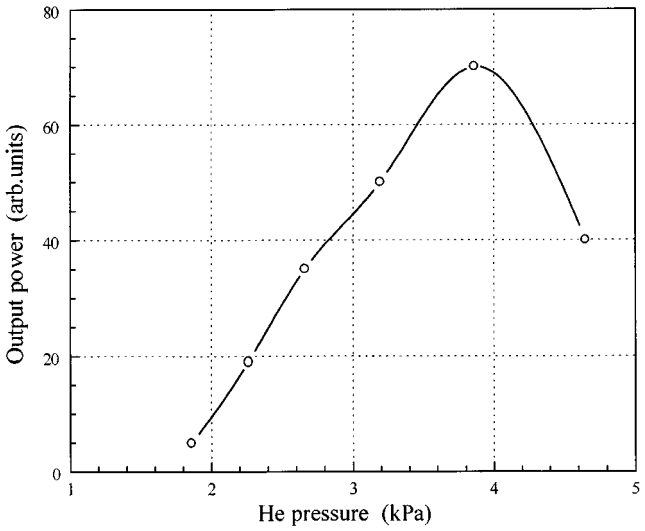

Fig. 6. Laser output power at $\lambda = 780.8$ nm Cu^+ as a function of He pressure. Excitation: RF = 27.12 MHz, amplitude of the power pulses = 750 W.

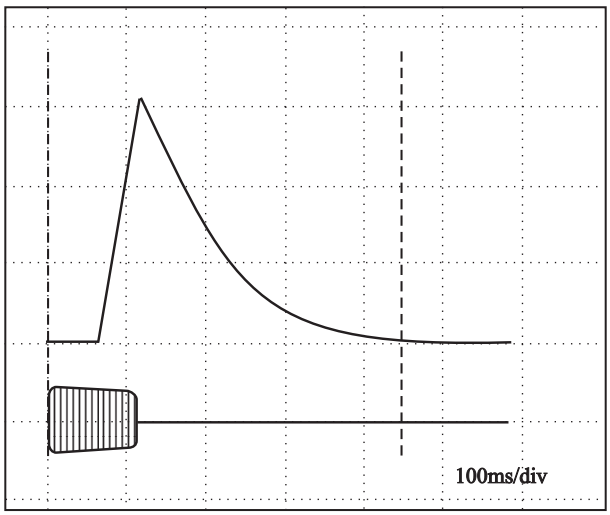

Fig. 7. Time behaviour of the RF (27.12 MHz) excitation pulse (lower course) and laser pulse at $\lambda = 780.8$ nm Cu^+ in the He–CuBr laser. Time scale = 100 μs/div.

the laser threshold Cu^+ ion concentration. The maximum amplitude of the laser pulse was always at the end of the excitation pulse and it increased with increasing excitation pulse duration. In the RF pulse duration range used in this experiment (from 40 μs to 120 μs) we did not reach any saturation of the laser pulse amplitude which means that the optimum Cu^+ ion density has been never obtained by us. After the RF pulse a long afterglow lasing, lasting up to 300 μs was observed.

The lowest amplitude of the RF input power pulses, at which the lasing was obtained, was about 500 W, corresponding to 12.5 W/cm of the linear RF power density. This value is much lower than the 100 W/cm, necessary for lasing in the sputtered RF-excited He–Cu system [13]. At the optimal He pressure of 4.0 kPa and 750 W pulse power

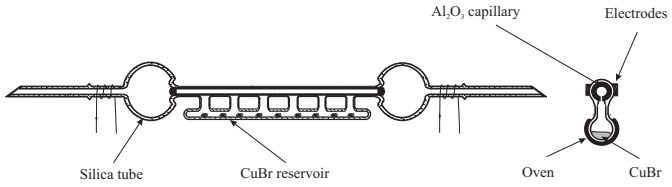

Fig. 8. Discharge tube for a RF-excited CuBr-based Cu^+ laser with Al_2O_3 inset.

amplitude (18.75 W/cm) a small-signal gain of 780.8 nm Cu^+ laser line was 8%/m.

However, in this tube we did not obtain CW lasing because we could not independently optimise the CuBr vapour pressure and excitation power. We noticed a strong sputtering of the silica discharge tube during the operation, which gradually deteriorated the discharge.

4.3 CW oscillation in He–CuBr discharge

To optimise the CuBr vapour pressure independently of the RF excitation power we developed a discharge tube, the design of which was based on the tube used for the RF-excited He–Cd^+ laser [11]. The discharge tube (Fig. 8) was made of fused silica. A capillary tube made of Al_2O_3 ceramic, 400 mm long and 4 mm inner diameter, was inserted into the centrally placed fused silica capillary tube, forming the active part of the laser tube. Using the Al_2O_3 capillary tube allowed lowering the sputter-originated problems [12] (met also in the experiment described in Sect. 3.2). The solid CuBr pieces were placed in a sidearm reservoir. Owing to it the CuBr vapour pressure in the active part of the laser tube could be controlled independently of the RF excitation power by separate heating of the reservoir. The CuBr sidearm reservoir was formed by a tube, extending parallel to the discharge tube and connected to the discharge volume with six vapour feedings, instead of one like in [11]. This was made to improve CuBr vapour distribution in the discharge volume. Two high reflecting mirrors with 1.5 m radii of curvature, set about 90 cm, formed the laser resonator apart. The He–CuBr discharge was excited with 13.56 MHz RF power.

CW simultaneous laser oscillation on four near-IR Cu^+ transitions at 740.4 nm, 766.5 nm, 780.8 nm and 782.6 nm was obtained. The highest laser output power was obtained on the 780.8 nm line, followed by the 740.4 nm line. The other two lines, 766.5 nm and 782.6 nm were comparatively weak and needed rather high excitation power.

The operating characteristics of the CW oscillations on the near-IR lines were measured under single line operation mode using a set-up, similar to that described in [11]. To separate each laser line a birefringent Lyot filter [29] together with a computerised assembly was placed in the resonator. The assembly consisted of two contra-rotating Fresnel plates producing either a variable output coupling or insertion loss for measuring the small-signal gain on the laser transition, and of a Fresnel plate tilted near the

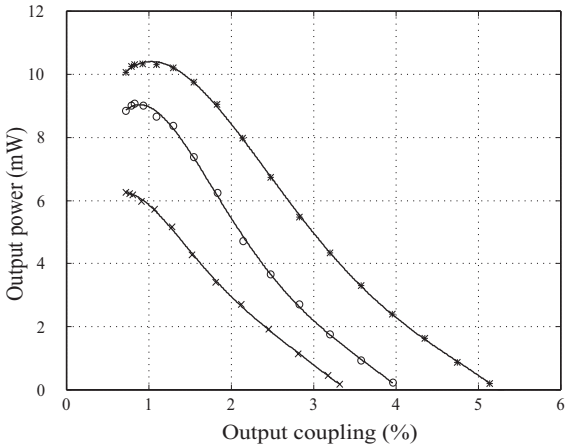

Fig. 9. Laser output power at $\lambda = 780.8$ nm Cu^+ as a function of output coupling for different RF input powers: (×) 600 W, (○) 700 W, (∗) 800 W.

Brewster angle to decouple a small part of the laser intra resonator power for recording the laser intra-resonator power. Taking into account the output coupling of the two contra-rotating and the fixed Fresnel plates, the total output coupling of the laser intra-resonator power could be calculated. The laser output power as a function of output coupling was determined from the product of the measured laser intra-resonator power and the total output coupling. All measurements were carried out at the optimal for laser operation temperature of the CuBr reservoir of 730 K, corresponding to a CuBr partial pressure of 12 Pa.

Figure 9 shows the laser output power at $\lambda = 780.8$ nm Cu^+ as a function of output coupling for different RF input powers. He pressure dependencies of the RF-excited CuBr laser output powers at $\lambda = 740.4$ nm and $\lambda = 780.8$ nm, when oscillating separately, are shown in arbitrary units in Figure 10. The laser output power at $\lambda = 780.8$ nm was four times higher than that at $\lambda = 740.4$ nm. The laser output power dependencies at $\lambda = 740.4$ nm and the $\lambda = 780.8$ nm exhibit narrow maxima around 5.2 kPa and 7.4 kPa, respectively. Such a different pressure dependencies of both laser lines are surprising since they have a common upper level. The laser output power at both lines increased with increasing RF input power and no saturation of the laser output power was reached up to 800 W RF input power, which was the limit of the RF generator (Fig. 11). The threshold RF input power for the laser oscillation on the 780.8 nm Cu^+ line was about 350 W, which corresponded to only 9 W/cm. The threshold RF input power for the laser oscillation on the 740.4 nm Cu^+ line was higher (480 W, corresponding to 12 W/cm). At the optimum conditions (He pressure of 7.4 kPa, CuBr reservoir temperature of 730 K and RF input power of 800 W) a laser output power of 10 mW at $\lambda = 780.8$ nm was obtained (Fig. 12). At these conditions the small-signal gain on 780.8 nm Cu^+ line was nearly 7%.

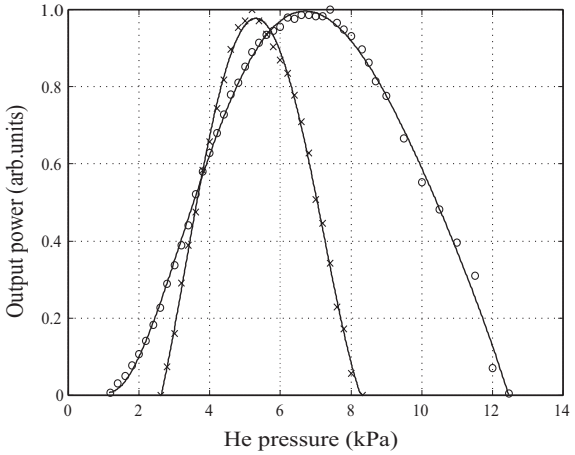

Fig. 10. Laser output power at $\lambda = 780.8$ nm ($\circ$) and $\lambda = 740.4$ nm ($\times$) as a function at He pressure. CuBr reservoir temperature = 730 K, RF input power = 600 W.

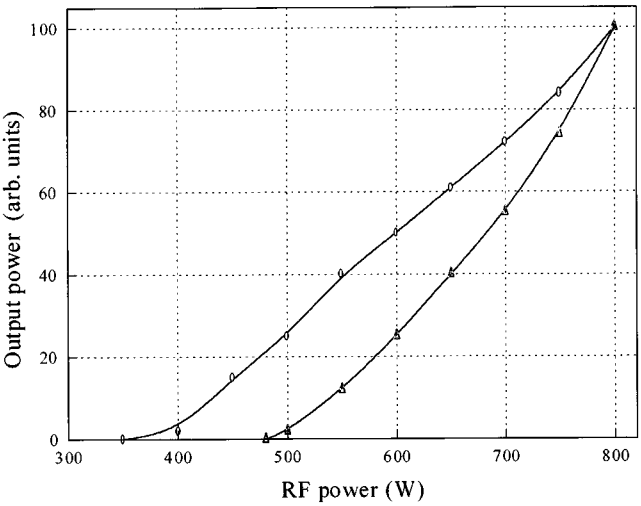

Fig. 11. Laser output power at $\lambda = 780.8$ nm ($\circ$) and $\lambda = 740.4$ nm ($\triangle$) as a function at RF input power at He pressure optimal for each line, CuBr reservoir temperature = 730 K.

5 Excitation of UV Cu^+ laser lines in RF-excited Ne–CuBr discharge

Using Ne as a buffer gas in the laser tube employed for the IR laser generation (Fig. 8), we tried to obtain laser oscillation in the UV spectral region. The pressure of Ne was varied from 0.1 kPa to 8.5 kPa. The CuBr reservoir temperature was 730 K (like in the He–CuBr discharge, Sect. 4). The Ne–CuBr discharge was excited with the 13.56 MHz RF generator. The laser resonator was formed by two high reflecting UV mirrors (246 ÷ 280 nm spectral range) with 2 m radii of curvature. The UV radiation emitted by the RF-excited Ne–CuBr discharge was measured *via* one of the mirrors (the front mirror) by a monochromator of high spectral resolution (Sopra UHRS F1150, equipped with a premonochromator and an Echelle-grating) with a photomultiplier.

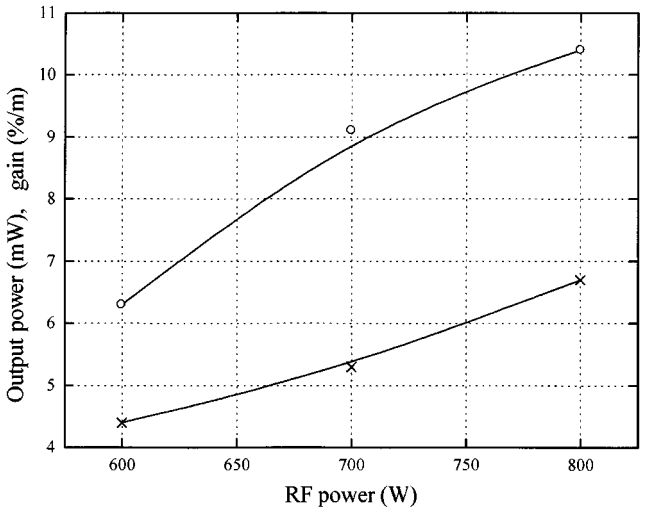

Fig. 12. Laser output power and small-signal gain at $\lambda = 780.8$ nm as a function of RF input power. He pressure = 7.4 kPa, CuBr reservoir temperature = 730 K.

28 UV Cu^+ lines with wavelengths between 240 nm and 274 nm were found in the measured spectra. The intensities of these lines were measured twice, first when the back resonator mirror was blocked with a shutter (intensity I_0) and then when the shutter was removed such that the discharge radiation could reflect from the back mirror (intensity I). The ratio I/I_0 for most measured UV lines is shown in Figure 13. Enhancement in the intensities of 14 Cu^+ lines was observed when the back mirror was active (not blocked), while the intensities of the rest Cu^+ lines remained unchanged when the back mirror was blocked and off-blocked. Only for 11 lines the enhancement in the intensity was more than twice (up to five times). This effect we recognise as a weak laser gain existing for these 11 UV lines of Cu^+ ion in the RF-excited Ne–CuBr discharge. It is known that laser oscillations on 9 of these UV lines were earlier obtained in a sputtering HC Ne–Cu discharge [1].

The Ne pressure dependencies of the spontaneous emission intensity of the two most intensive Cu^+ lines, $\lambda = 248.6$ nm and $\lambda = 260.6$ nm, are presented in Figure 14. Both lines exhibit a maximum at Ne pressure of about 1 kPa.

Although we observed a laser gain for 11 UV Cu^+ lines in the RF-excited Ne–CuBr discharge, we were not able to obtain laser oscillation even at the optimum conditions. Apparently, even at the highest available RF input power (800 W) the gain was not high enough to compensate the losses for the UV laser lines, which usually are relatively high.

6 RF-excited He–CuBr IR laser with cataphoretic vapour transport

We found that one of the most important obstacles to efficient operation of the RF-excited He(Ne)–CuBr discharges is the inhomogeneous distribution of the CuBr

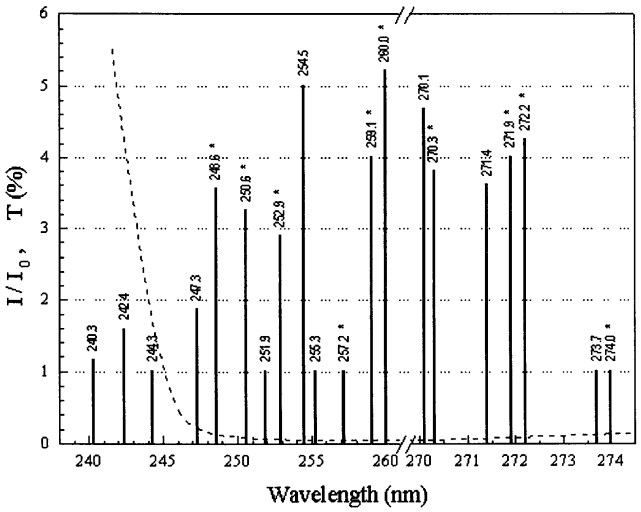

Fig. 13. Ratio I/I_0 for most of the measured UV Cu^+ lines in the RF-excited Ne–CuBr discharge. Ne pressure = 1 kPa, CiBr reservoir temperature = 730 K, RF input power = 600 W. Laser lines are marked by (∗). Dashed line: the transmittance of the laser mirrors.

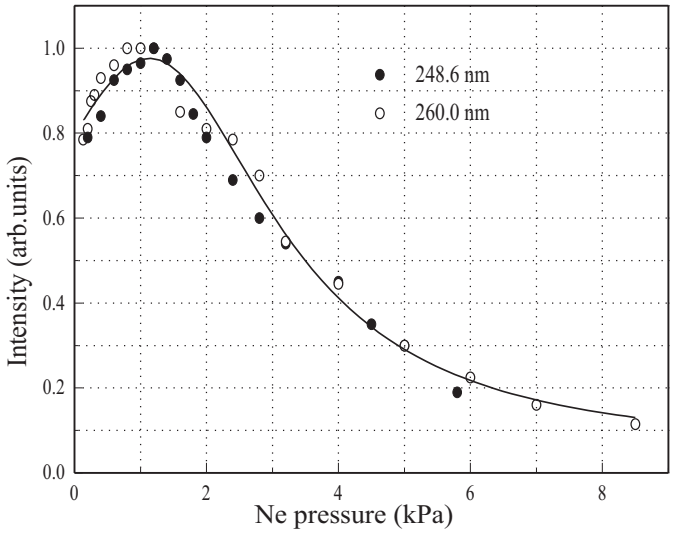

Fig. 14. Intensity of 248.6 nm and 260.0 nm Cu^+ lines as a function of Ne pressure. CuBr reservoir temperature = 730 K, RF input power = 600 W.

vapour along the discharge length. Apparently, due to the poor diffusion of CuBr vapour (although we used in our experiments a special design of the CuBr reservoir (Fig. 8), delivering CuBr vapour in several places along the discharge length), we never obtained a uniform axial distribution of the CuBr vapour.

For improving the CuBr vapour distribution along the discharge length we employed cataphoresis, similarly to Goldsborough [30], who used cataphoresis to obtain uniform distribution of Cd^+ ions in a positive column He–Cd^+ laser. We superimposed a DC current, causing the cataphoresis on the transverse RF discharge and run both discharges simultaneously in a tube, supplemented with

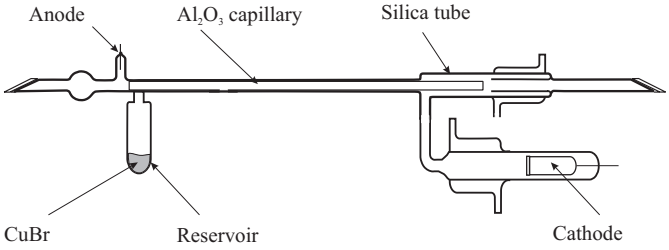

Fig. 15. He–CuBr laser tube with cataphoretic vapour transport.

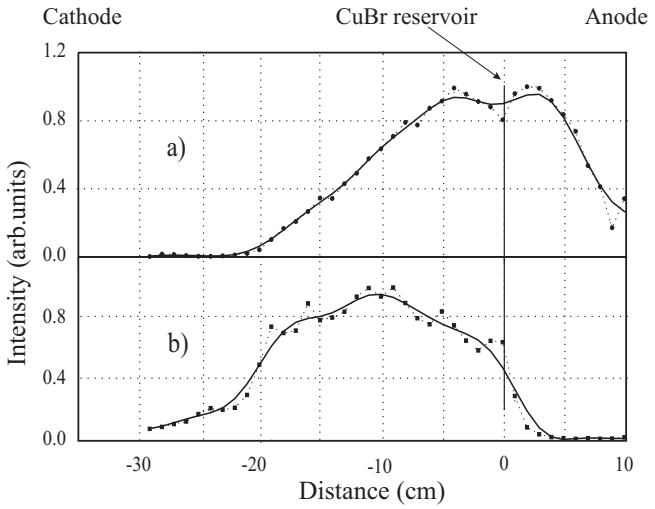

Fig. 16. Intensity of the 521.8 nm Cu atomic line along the discharge length in the CuBr laser tube: (a) without cataphoresis (RF), (b) with cataphoresis (RF and DC superimposed); He pressure = 10 kPa, CuBr reservoir temperature = 730 K, RF power = 600 W, DC discharge current = 20 mA.

a conventional DC anode and cathode, and a side-arm reservoir with CuBr, placed at the anode side (Fig. 15).

To compare the Cu vapour distribution along the discharge length at only RF and at simultaneous RF and DC excitation, the axial intensities of the emission of the strongest Cu and Cu^+ lines were recorded. Figure 16 shows the intensity of 521.8 nm Cu atomic line along the discharge length at RF excitation (without cataphoresis) and at simultaneous RF and DC excitation (with cataphoresis). A similar behaviour was observed for the intensity of 780.8 nm Cu^+ line. Assuming in the first approximation proportionality between the intensity of 521.8 nm Cu line and Cu atom density, we interpret Figure 16 as follows. An essential decrease of the Cu atoms density between the oven and the cathode observed at the RF excitation (without cataphoresis, Figure 16, curve a) is typical of diffusion controlled transport of an admixture in the discharge without cataphoresis [31]. On the other hand, when an additional current of 20 mA was superimposed on the RF discharge, the resulting electric DC-field caused an efficient transport of the copper vapour towards the cathode, which is indicated by more uniform axial distribution of 521.8 nm Cu line intensity (Fig. 16, curve b).

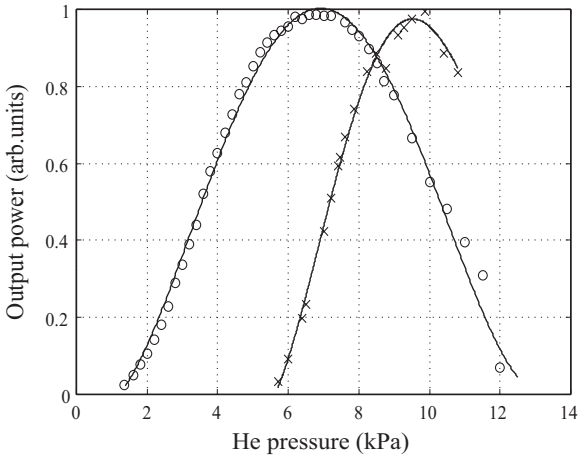

Fig. 17. Laser output power at $\lambda = 780.8$ nm as a function of He pressure. (○) RF excitation, (×) RF and DC excitation, the power should be multiplied by 2. CuBr reservoir temperature = 730 K, RF power = 600 W, DC discharge current = 20 mA.

Using this laser tube laser oscillation on 780.8 nm Cu^+ line was obtained with both the RF excitation and the superimposed RF and DC excitation. The laser output power increased by a factor of two when cataphoresis due to the DC discharge exist. The simultaneous RF and DC excitation shifted the He pressure optimum for lasing from 7 kPa to 10 kPa (Fig. 17). A similar effect was also observed for the He–Cd^+ laser [32] excited by simultaneous RF and DC discharge. The lower optimum He pressure in the RF-excited He–CuBr (and also He–Cd^+) laser, *i.e.* without cataphoresis, is a result of a slower diffusion-controlled transport of Cu (or Cd) vapour from the CuBr (or Cd) reservoir along the laser tube at higher He pressures. This results in a Cu vapour distribution along the laser tube worse than that at lower He pressures, whereby at higher He pressures the laser operation is hampered. On the other hand, under the cataphoresis operation the Cu vapour distribution along the laser tube preserves its better uniformity at higher He pressures, resulting in a higher laser output power, as shown in Figure 17. The doubled laser output power at $\lambda = 780.8$ nm under the cataphoresis operation is caused by two factors, first, the better Cu vapour axial distribution, and second, the higher He pressure, which results in a higher concentration of He^+ ions involved in the excitation of Cu atoms to the upper laser states (reaction (1)).

In this experiment we also observed that the DC current superimposed on the RF discharge stabilises it. This is another factor showing that superimposing the RF and DC discharge is a promising solution when an efficient CuBr-based laser is considered.

7 Conclusions

In these experiments it was shown that utilizing CuBr mixture as a source of Cu atoms for the RF discharge can be a promising alternative to the Cu sputtered system, when the development of Cu ion gas lasers is considered. When using the CuBr mixture, the RF discharge is needed only for dissociation of the CuBr molecules to obtain Cu atoms in the discharge volume, and for exciting them to the laser states. The heat dissipated during the concurrent discharge processes is enough to keep the system in a temperature appropriate for vapourising the CuBr mixture. Therefore, the CuBr-based laser system is capable of avoiding the high input power needed for the Cu sputtered systems.

Both our spectroscopic and laser investigations showed that the threshold input power for lasing was reduced about 5 times using the CuBr-based system (about 15–20 W/cm) instead of the Cu-sputtered system (100 W/cm).

The pulsed and CW laser oscillations on four infrared Cu^+ transitions ($\lambda = 740.4$ nm), 766.5 nm, 780.8 nm, 782.6 nm) were obtained in the RF-excited He–CuBr discharge operated at 13.56 MHz and 27.12 MHz.

At an optimum He pressure of 7 kPa, temperature of CuBr reservoir of 730 K and input RF power of 800 W, an output power of 10 mW at the strongest Cu^+ laser line $\lambda = 780.8$ nm was achieved. A better Cu vapour axial distribution and better discharge stability was achieved when DC discharge was superimposed on the RF discharge, which resulted in increase of laser output power by a factor of two.

A laser gain for 11 UV Cu^+ lines was observed in Ne–CuBr RF-excited discharge. Although we did not obtain laser oscillation in the UV range, basing on the obtained results, we consider the CuBr laser system excited by RF discharge capable of generating UV laser radiation at relatively low input power.

This work was supported by the European Commission Copernicus Programme CIPA-CT 93-0219 and the NATO Science for Peace Programme SfP 971989. Parts of the investigations were supported also by the Bulgarian Science Fund, Grant F-702.

References

1. I.G. Ivanov, E.L. Latush, M.F. Sem, *Metal Vapour ion Lasers: Kinetic processes and Gas Discharges*, edited by C.E. Little (John Wiley & Sons, 1996), p. 256.
2. D.C. Gerstenberger, R. Solanki, G.J. Collins, IEEE J. Quant. Electron. **QE-16**, 820 (1980).
3. M. Yang, Appl. Phys. B **32**, 127 (1983).
4. C.S. Liu, E.W. Sucov, L.A. Weaver, Appl. Phys. Lett. **23**, 92 (1973).
5. C.J. Chen, N.M. Nerheim, G.R. Russell, Appl. Phys. Lett. **23**, 514 (1973).
6. N. Sabotinov, *NATO Advanced Research Workshop on Pulsed Metal Vapor Lasers - Physics and Emerging Applications in Industry, Medicine and Science*, St. Andrews, UK, edited by C.E. Little, N. Sabotinov (Kluwer Academic Publishers, 1995), p. 113.
7. R. Solanki, W.M. Fairbank Jr, G.J. Collins, IEEE J. Quant. Electron. **QE-16**, 1292 (1980).
8. H.J. Eichler, H. Koch, R. Molt, J.L. Qiu, Appl. Phys. B **26**, 49 (1981).

9. J. Mizeraczyk, J. Mentel, N. Sabotinov, Proc. SPIE **3052** 17 (1996).
10. J. Mentel, N. Reich, J. Mizeraczyk, M. Grozeva, N. Sabotinov, *NATO Advanced Research Workshop, Gas lasers - recent Developments and Future Prospects*, Moscow, edited by W.J. Witteman, V.N. Ochkin (Kluwer Academic Publishers 1995), p. 55.
11. N. Reich, J. Mentel, J. Mizeraczyk, IEEE J. Quant. Electron. **QE-31**, 1902 (1995).
12. N. Reich, J. Mentel, G. Jakob, J. Mizeraczyk, Appl. Phys. Lett. **64**, 397 (1994).
13. V. Mikhalevskii, M. Sem, G. Tolmachev, V. Khasilev, J. Appl. Spectr. **32**, 321 (1980).
14. M. Grozeva, N. Sabotinov, Proc. SPIE **3052**, 131 (1996).
15. M. Kocik, J. Mizeraczyk, M. Grozeva, N. Sabotinov, J. Mentel, J. Schuze, D. Teuner, T. Adamowicz, Proc. SPIE **3186**, 228 (1996).
16. J.A. Piper, D.F. Neely, Appl. Phys. Lett. **33**, 621 (1978).
17. E. Webb, A.R. Turner-Smith, J.M. Green, J. Phys. B: At. Mol. Phys. **3**, L134 (1970).
18. M. Kocik, D. Grabowski, J. Mizeraczyk, J. Heldt, J. Schulze, J. Mentel, *ICPIG XXIII*, Toulouse, France, 1997, p. 50.
19. M. Kocik, J. Schulze, D. Teuner, M. Grozeva, D. Grabovski, J. Heldt, J. Mizeraczyk, J. Mentel, *Intern. Symposium on Plasma Research and Application, PLASMA'97* (Jarnotówek near Opole, Poland, 1997), p. 275.
20. J. Mizeraczyk, W. Urbanik, J. Phys. D: Appl. Phys. **16**, 2119 (1983).
21. Ch. Herzberg, *Spectra of Diatomic Molecules; Molecular Spectra and Molecular Structure* (Van Nostrand Reinholds Company, 1950).
22. P. Gill, C.E. Webb, J. Phys. D: Appl. Phys. **10**, 299 (1977).
23. V. Khasilev, V. Mikhalevskii, G. Tolmachev, Sov. J. Plasma Phys. **6**, 236 (1980).
24. Yu.P. Reizer, *Gas discharge physics* (Springer-Verlag, Berlin Heidelberg, 1991), p. 378.
25. A. Passchier, J. Christian, N. Gregory, J. Phys. Chem. **71**, 937 (1967).
26. Hideo Okabe, *Photochemistry of Small Molecules* (A Wiley-Intersci. Publ., John Wiley and Sons, NY 1980), p. 221.
27. D. Astadjov, N. Vuchkov, G. Petrash, N. Sabotinov, *Proceedings of the Lebedev Physics Institute - Metal vapor and metal halide vapor lasers*, edited by G.G. Petrash (Nova Science Publishers, Moscow, 1987), p. 183.
28. N. Reich, Ph.D. thesis, Ruhr Universitat, Bochum, Germany, 1994.
29. J. Mentel, E. Schmidt, T. Mavrudis, Appl. Optics **31**, 5022 (1992).
30. P. Goldsborough, Appl. Phys. Lett. **15**, 159 (1969).
31. T.P. Sosnowski, J. Appl. Phys. **40**, 5138 (1969).
32. D. Teuner, J. Schulze, E. Schmidt, J. Mentel, *XXIII ICPIG*, Toulouse, France, 1997, p. 30.